IAES International Journal of Artificial Intelligence (IJ-AI)
Vol. 15, No. 2, April 2026, pp. 1143~1154
ISSN: 2252-8938, DOI: 10.11591/ijai.v15.i2.pp1143-1154

Multi-dimensional performance-optimized array design framework for efficient mmWave energy harvesting

Shalini Mirle Gajendra[1,2], Naveen Kalenahalli Bhoganna[3]
[1]BGS Institute of Technology, Adichunchanagiri University, Bellur, India
[2]Department of Electronics and Communication Engineering, Dayananda Sagar Academy of Technology and Management, Bangalore, India
[3]Department of Electronics and Communication Engineering, BGS Institute of Technology, Adichunchanagiri University, Bellur, India

Article Info

Article history:

Received Aug 14, 2025
Revised Jan 12, 2026
Accepted Jan 25, 2026

Keywords:

Energy–information optimization
Integrated analog–digital beamforming
mmWave energy harvesting
Multi-dimensional array design
Resource optimization algorithms

ABSTRACT

The proliferation of next-generation wireless networks and autonomous devices has intensified the need for efficient and compact energy harvesting solutions at millimeter-wave (mmWave) frequencies. This paper presents a multi-dimensional performance-optimized array design framework for mmWave energy harvesting (MAPLE-H), which enables the systematic development of advanced antenna arrays that fulfill the simultaneous demands of wide operational bandwidth, high efficiency, polarization diversity, and miniaturization. The proposed framework integrates simulation-driven array modeling with integrated analog–digital beamforming and adaptive entity partitioning, accommodating real-world energy harvesting array non-idealities. Furthermore, an energy–information optimization factor is introduced to dynamically balance the trade-off between energy harvesting and data communication performance. Intelligent energy–information resource optimization algorithms jointly tune design parameters to maximize harvested power and signal integrity across diverse deployment scenarios. Comprehensive simulation results and comparative benchmarking demonstrate that the proposed framework consistently outperforms state-of-the-art designs in terms of gain, bandwidth, robustness, and flexibility, positioning it as an enabling technology for future energy-autonomous wireless systems.

Corresponding Author:

Shalini Mirle Gajendra
BGS Institute of Technology, Adichunchanagiri University
Bellur, B. G. Nagar, India
Email: shalini_180701@rediffmail.com

1. INTRODUCTION

The fast growth of next-generation wireless communication technologies, especially those that work in the millimeter-wave (mmWave) spectrum, has created both exciting prospects and big problems for the design of devices and infrastructure that support them. The use of the spectrum has moved into higher frequency bands, such 24 GHz, 28 GHz, 38 GHz, and higher, as 5G and 6G systems have developed. This is because these bands can offer faster data speeds, reduced latency, and wider channel capacity. These high-frequency bands are good for ultra-reliable and low-latency communication, but they also have higher propagation loss and require more advanced antenna systems to work well in all situations [1].

As communication systems have gotten better, there has also been a rising demand for energy-efficient solutions to handle the huge number of devices that are linked to wireless networks. Wearable sensors, embedded medical devices, autonomous sensors in smart environments, and low-power

internet of things (IoT) modules are just a few examples of applications that need wireless, battery-free power sources. Ambient radio frequency (RF) energy harvesting is one very promising way to address this need. RF energy harvesting lets devices take electromagnetic energy from ambient signals and turn it into useable electrical power. This is different from traditional energy sources that need cable connections or batteries that need to be changed often. Researchers are now more interested in combining energy harvesting with communication subsystems, especially in devices that will be used in crowded mmWave-enabled urban and industrial areas [2].

The antenna is the most important part of any RF energy harvesting system. It serves two purposes: it is a communication device and a power acquisition front-end. In energy-harvesting applications, the antenna needs to work well throughout the necessary frequency range and also collect as much RF energy as possible. To do this, the system has to have features like high gain, a wide impedance bandwidth, good radiation efficiency, and steady directional coverage. Antenna systems must be designed particularly for high-frequency propagation to efficiently support mmWave energy harvesting. This is because high-frequency propagation has a lot of free-space path loss, little diffraction, and is easy to block [3].

Antenna arrays, especially those made for mmWave bands, have several great benefits that can help get around these problems. Antenna arrays can provide better directivity, gain, and spatial resolution by putting together many radiating elements in a phased or geometrically optimized way [4]. These features are important not only for the quality of communication but also for getting the most energy from RF sources in the environment. For energy harvesting, arrays may be made even better by adding polarization variety (such circular or dual-polarized components), beam-steering capabilities, and smart array structure to make them work better in electromagnetic environments that change all the time [5].

The change to mmWave frequencies has made antenna array design more complicated. Because the wavelengths are shorter, it's possible to fit more antenna components into a small space. This makes high-gain arrays useful even for small devices like wearables or embedded devices. However, this advantage is canceled out by the fact that it is more sensitive to alignment, angle of incidence, and reflections from the surroundings. So, mmWave antenna arrays for energy harvesting need to be built to not only have the most gain in one direction, but also to work well at a wide variety of angles and polarizations. This makes sure that devices keep working even when they aren't exactly lined up with the source or when they are moving. The literature has looked at a number of design solutions to get around these problems. In situations where ambient energy is being collected, circularly polarized (CP) antennas are generally preferred since they can keep working well no matter which way signal is coming from. This is especially helpful in circumstances that change. Multibeam and multiband antenna setups also let you cover a wider range of frequencies and collect energy from more than one source at same time. Using dielectric lenses, metamaterials, and resonant structures can boost gain and angle coverage even more without making design any more complicated [6].

In addition to physical design, modeling and analysis are very important for making high-performance mmWave energy harvesting antennas. Researchers can use electromagnetic simulation tools like CST Microwave Studio, Ansys HFSS, and MATLAB-based modeling frameworks to study how antennas function in controlled settings, improve design parameters, and test theoretical performance before making physical prototypes. These simulation tools let you simulate gain, return loss, radiation efficiency, and other important aspects in full wave. They also make it possible to analyze more complex setups like phased arrays, adaptive beamforming, and multi-input rectifier loading. Each of these can help improve the system's capacity to collect energy. Along with optimizing specific devices, mmWave antenna arrays are also being looked at more and more for their potential to gather energy throughout the whole network. When there are several RF sources in the same area, including base stations, relays, and access points, the way RF energy is spread out in space is more complicated. Antenna arrays that can adaptively respond to these changes through dynamic beam shaping, adaptive entity partitioning, or signal combining algorithms provide you a strategic edge. In addition, adding reconfigurable or software-defined features, such as hybrid analog-digital precoding or clever reflector-assisted setups, makes energy harvesting systems even more useful, especially in smart city or vehicle applications. Building these kinds of systems in real life is still hard because of how complicated they are to make and how hard it is to put them together, but much of the new ideas and testing that is happening right now is happening through software-defined simulations. This method lets researchers look at a lot of different configurations, frequency ranges, and optimization methodologies without having to pay for and wait for hardware prototypes. As simulation tools get better, antenna designers may mimic real-world situations including multi-path propagation, urban clutter, user movement, and changes in angle of an incident wave. This makes simulation-based analysis a useful and complete way to create antennas [4].

As more and more people want devices that can run on their own and connect to the internet wirelessly, the combination of mmWave technology with ambient RF energy harvesting is an especially important field of research. The basis for this convergence is antenna arrays that have been designed just for collecting energy [7]. It is feasible to create antennas that not only provide reliable communication but also

keep their energy autonomy in next-generation systems by carefully designing them, analyzing their performance, and optimizing them under realistic simulation scenarios. Using a simulation-first strategy to study mmWave antenna arrays is a viable way to get toward scalable, high-efficiency RF energy harvesting for advanced wireless applications.

Because 5G and 6G wireless technologies are moving so quickly, it is now necessary to use mmWave frequency bands to satisfy the needs for fast, high-capacity communication. At the same time, the expanding number of low-power wireless devices, such wearables, IoT sensors, and remote monitoring systems, has made it very important to find energy-autonomous solutions that don't rely on batteries or connected power sources. Ambient RF energy harvesting is a great option since it lets devices use electromagnetic energy that is freely accessible into usable electrical power [8], [9]. However, it is very hard to successfully gather energy at mmWave frequencies because of increasing path loss, limited beamwidths, and the fact that high-frequency signals only go in one way [10]. Standard single-element or fixed-beam antenna constructions have low gain, a narrow operational bandwidth, and limited flexibility, which makes them not the best choice for collecting dynamic ambient RF energy in real-world settings.

Also, some antenna designs have high gain or broad rods, but they can't always change to changes in signal direction, polarization, or correspondingly samplers, burling r in the, or environmental impediments. In smart city, mobile, or multi-source RF contexts where the angle of incidence and signal intensity are often changing, this static characteristic makes them less useful [11]. There is a big gap in research since there isn't a flexible, simulation-driven antenna array architecture that balances high gain, broadband operation, and adaptive beam control for mmWave RF energy harvesting. We need a simulated antenna array system that works well in the lab and also keeps its energy capture efficiency in different and unexpected RF environments, without having to rely on hardware development [12].

The fast expansion of IoT, wearables, and wireless sensor networks has made the need for systems that can run on their own energy even greater. Using batteries makes things harder to scale, requires more upkeep, and raises environmental problems. Ambient RF energy harvesting is a long-term solution that turns electromagnetic energy that is already around us into useful electricity. 5G and beyond use mmWave frequencies, which means there is a lot of RF energy in the air. But mmWave bands have significant path loss, small beams, and are sensitive to direction, therefore antenna systems need to be high-gain, wideband, and able to change with the circumstances. Most current harvesting antennas are either fixed-pattern, narrowband, or reliant on technology, which makes them less useful in real-world settings where conditions change. This makes it necessary to use simulations to develop and improve mmWave antenna arrays that can efficiently collect RF energy in a wide range of frequencies and directions. Simulation lets you test different array shapes, beamforming methods, and performance metrics without being limited by hardware. This makes it a great tool for designing the next generation of self-powered devices.

Development of an energy–information optimization factor integrated complementary antenna for mmWave energy harvesting. This work introduces a novel complementary antenna array architecture enhanced with an energy–information optimization factor mechanism that enables efficient multi-dimensional performance-optimized array design framework for mmWave energy harvesting (MAPLE-H). The design achieves high peak gain (PG) of 25.1 dBic, broad axial ratio bandwidth (ARBW) of 26.9%, and radiation efficiency (~90%) over a wide mmWave spectrum (32–44 GHz). Unlike conventional bulky designs, the proposed model maintains a compact structure with only three PCB layers, supporting manufacturability and cost efficiency for smart city and IoT deployments.

Simulation-based mmWave nonorthogonal multiple access (NOMA) system incorporating joint precoding and adaptive entity partitioning. The study proposes an iterative hybrid analog/digital precoding strategy for a mmWave multiple-input multiple-output (MIMO)-NOMA framework that facilitates user clustering and beamforming with channel state information (CSI)-driven optimization. It uses cluster head selection (CHS) and zero forcing (ZF) digital precoding to mitigate intra- and inter-beam interference. The method integrates hardware impairments and energy–information optimization factor noise into the signal-to-interference-plus-noise ratio (SINR) model and uses a minimum mean square error (MMSE) transformation to formulate and solve a non-convex optimization problem balancing spectral and energy efficiency.

Joint optimization framework for power allocation and energy harvesting. The research presents a joint power allocation and energy–information optimization factor optimization framework that maximizes the achievable sum rate (ASR) while satisfying constraints on minimum data rate and harvested energy thresholds. By iteratively updating the MMSE and convexifying constraints via Schur complements and auxiliary variables, the system achieves robust performance under practical mmWave impairments. This methodology enhances system efficiency for energy-constrained next-generation wireless environments, providing a scalable approach for integrating energy harvesting in dense urban wireless networks.

2. RELATED WORK

mmWave energy harvesting has rapidly gained traction as a critical enabler for powering autonomous devices in 5G and beyond wireless systems. The unique characteristics of mmWave propagation—such as high path loss, directionality, and sensitivity to obstructions—demand innovative antenna architectures that go beyond traditional energy-harvesting models. Early research primarily focused on single-element antennas or narrowband systems that struggled to maintain sufficient energy collection in dynamic urban settings. These limitations led to an increased focus on antenna arrays, especially those employing circular polarization and broadband features, to improve performance in terms of impedance matching, gain, and angular diversity [13].

To address the need for robust energy capture in variable conditions, several studies have explored CP antenna arrays. However, most conventional designs—like patch or dielectric resonator antennas (DRAs)—suffer from limited ARBW, often under 30%. For example, patch arrays enhanced with sequential rotation techniques can offer moderate improvements, but the overlap between axial ratio and impedance bandwidth typically falls short of the demands of practical mmWave environments. DRAs, while capable of broader bandwidth, often involve complex fabrication processes and high costs, limiting their scalability for widespread deployment [14].

To overcome these constraints, recent developments have emphasized novel configurations such as magneto-electric (ME) dipole arrays, integrated waveguide feeds, and complementary antenna structures. The ME dipole array developed by Feng *et al.* [15] incorporated substrate integrated waveguide (SIW) feeding mechanisms to achieve over 27% bandwidth in both axial ratio and impedance parameters. Still, rigid and multilayered nature of SIW-based solutions presents challenges in terms of design complexity and fabrication tolerance, particularly when implemented in high-density urban applications where spatial and cost constraints prevail. An important breakthrough came with the introduction of aperture-coupled complementary antenna structures, such as design proposed by Ji *et al.* [16], which demonstrated over 38% ARBW across 53–79 GHz range. These designs leverage complementary feed networks and optimized radiation patterns to enhance circular polarization without relying on external polarizers or bulky lenses. This approach aligns closely with demands of mmWave energy harvesting, especially for use cases in IoT and smart city contexts where compactness, cost-efficiency, and directional stability are vital [17].

In parallel, simulation-driven studies have begun exploring the integration of reconfigurable intelligent surfaces (RIS) to enhance energy coverage and harvested energy in mmWave networks. Saleh *et al.* [17] utilized a stochastic geometry framework to show that deploying passive RIS elements significantly improves energy harvesting metrics such as energy coverage probability (ECP) and average harvested energy (AHE), even under high path loss conditions. These findings suggest that RIS, when coupled with optimized antenna arrays, can form the foundation for spatially adaptive energy-harvesting networks with minimal power and structural overhead [18].

Several real-world implementations have also validated the feasibility of broadbeam and multibeam antenna systems for high-efficiency RF-to-DC conversion. Joshi *et al.* [19] introduced a 25-pixel CP rectenna integrated with a 3D equiconvex dielectric lens, achieving 6.5 mW power capture across wide angular coverage [20]. Similarly, Deng and Luk [21] developed a dual-polarized ME-dipole rectenna array with an integrated Luneburg lens to support 130° spatial coverage and 40% RF-to-DC efficiency across 24–40 GHz. These systems demonstrate that intelligent lens integration and multiband operation are essential for adapting to real-time variations in signal direction and strength, making them ideal for industrial and vehicular energy-harvesting use cases [22].

Another crucial direction in recent work involves the integration of MAPLE-H capabilities. Hybrid analog-digital precoding, as seen in NOMA-based MIMO systems, offers a dual-functional solution where the antenna not only harvests energy but also decodes information [23]. This has led to architectures that incorporate energy–information optimization factor (PS) mechanisms, enabling dynamic signal partitioning for energy and data streams. The effectiveness of such architectures hinges on real-time CSI and efficient adaptive entity partitioning strategies, making them inherently complex but highly efficient in spectral and energy domains [24].

In summary, while early research predominantly focused on standalone energy-harvesting antennas with fixed geometry, the current trend gravitates toward multi-functional, wideband, and adaptive systems driven by simulation-first methodologies. The incorporation of complementary antenna structures, RIS, MAPLE-H capabilities, and integrated analog–digital beamforming schemes represents a paradigm shift in mmWave energy harvesting research [15], [25]. These innovations not only expand the operational bandwidth and gain of the systems but also ensure resilience against dynamic urban propagation environments, positioning them as key enablers for future self-sustaining IoT networks [16].

3. METHOD

Upon careful consideration the hybrid precoded mm-wave huge point-to-point MIMO NOMA system is formulated. It needs precoder design and power allocation scheduling based on CSI. There are channels that are strongly linked in the same direction and the highly focused beams of the large-scale antenna in mm-wave enable NOMA deployment in each beam for greater beamforming gains and reduced inter-beam interference compared to their OMA equivalents. The fully linked and sub-connected hybrid architectures with energy harvesting capabilities for downlink communication and uplink channel estimation are considered, you might be able to apply ideas to make the job better for users with more than one antenna, difficult CHS for adaptive entity partitioning, and analog/digital precoding. Figure 1 shows joint precoding and MAPLE-H-based resource allocation framework for mmWave MIMO-NOMA

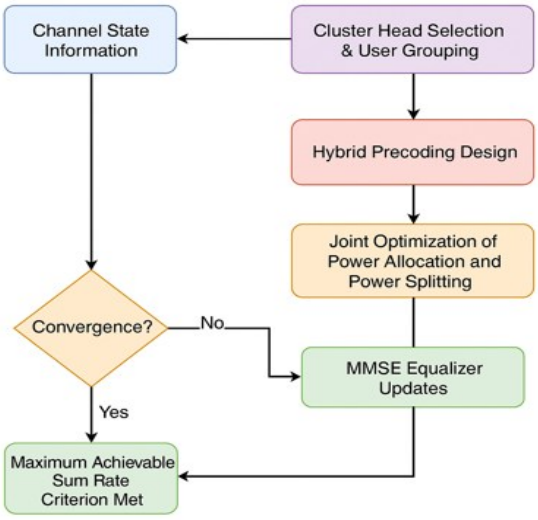

Figure 1. Joint precoding and MAPLE-H-based resource allocation framework for mmWave MIMO-NOMA

The transceiver system is modelled via a single cell such that the number of RF chains P_{RF} is used fully through equal number of beams, rays and cluster groups P_E. The set of users in a cluster is represented by W_e, $e = 1,2, \dots, E$ by denoting that $w_k \cap w_l = \text{null}, \text{k} \neq \text{l}$, $|W_e| \geq 1$ and $\sum_{e=1}^{E} |W_e| = \text{m}$. For downlink user detection, we assume an uplink initial CSI, which is the received signal vector $a_e \in E^{(Po \times 1)}$ at an arbitrary cluster e is represented as (1).

$$a_e = J_e^J R \sum_{k=1}^{e} \sum_{l=1}^{|w_k|} s_k \sqrt{x_{k,l} u_{k,l}} + p_e \quad (1)$$

Where J_e denotes the channel matrix of P_D by P_O per cluster. The adjacent downlink Gaussian noise vector is $p_e \in E^{(Po \times 1)}$. The analog precoding matrix $E^{(P_D \times P_E)}$ along with digital precoding as $s \in E^{(P_E \times 1)}$ for the cluster, e are relevant in the form $||Rs_e||_2 = 1$. The power transmitted within the $k - th$ cluster and $l - th$ user is $x_{k,l}$. The precoded architecture consists of two phases, the fully connected type $R^{(H)}$ denotes the spectral co-efficient connected to the type $R^{|U|}$ that is energy efficient in terms of number of radio frequencies mapped via transmitting antenna using $SE\ R^{(H)} = \left[r_1^{(H)}, r_2^{(H)}, \dots, r_E^{(H)}\right]$ with $r_e^{(H)} \in E^{(P_G \times 1)}$, the EE $R_E^{(U)} = bd[R_{F1}^{(U)}, R_{F2}^{(U)}, \dots\dots, R_{FE}^{(U)}]$ for $R_{Fe}^{(U)} \in E^{(P_{F_E} \times 1)}$ $e = 1,2, \dots \dots, E$ with vectors $P_{F_E}(\frac{P_D}{P_E})$ these rows are spanned across P_E or P_{RF} columns RF of an $(P_D \times P_E)$ block diagonal matrix. All clusters for either connection type have the same amplitude but distinct phases, channel models are designed as (2).

$$J_e = \sqrt{\frac{P_D P_O}{\sigma_e}} \sum_{k=1}^{N_e} \tau_e^{(n)} c_D\left(\theta_D^{(n)}\right) c_O\left(\varphi_O^{(n)}\right) \quad (2)$$

The number of paths for users in a cluster e is N_e ,each path is characterized by a high gain $\tau_e^{(n)}$, angle of departure (AOD), $\theta_D^{(n)}$, the angle of arrival as $\varphi_O^{(n)}$ and associated average path loss as σ_e is denoted

by the number of paths N_e. Clustering makes the statement easier to understand such that $P_D \times P_O$ channel matrix and $P_O \times 1$ noise vector is reduced by common size located P_O per user m in cluster e by reshaping the matrix. J_e assuming element-wise noise distribution in p_e assuming the similar element-wise noise vector reduced by the common size located as P_O per user m in cluster e by reshaping the matrix. J_e assuming element-wise noise distribution in p_e that obtains $j_{e,m}$ and $p_{e,m}$. The resultant channel model is expressed as (3) and (4).

$$j_{e,m} = \sqrt{\frac{P_D P_O}{N_{e,m}}} \sum_{k=1}^{N_{e,m}} \tau_{e,m}^{(n)} c^{(o)}\left(\theta_{e,m}^{(n)}\right)\left(\varphi_{e,m}^{(n)}\right) \tag{3}$$

$$\sum_{k=1}^{N_{e,m}} b_{e,m}^{(n)} c_D\left(\theta_{e,m}^{(n)}\right)\left(\varphi_{e,m}^{(n)}\right) \tag{4}$$

Here $b_{e,m}^{(n)} = \sqrt{\frac{P_D P_O}{N_{e,m}}} \sum_{k=1}^{N_{e,m}} \tau_{e,m}^{(n)}$, and $c_D\left(\theta_{e,m}^{(n)}\right)\left(\varphi_{e,m}^{(n)}\right)$ by steering vector projected onto one antenna out of P_O antennas that are selected and randomly indexed o for all M users. The received signal at the $m-th$ user is denoted as (5) wherein the expressions on to the right of equal sign stand for the intra-beam interference, inter-beam interference, and noise signals, in that order. The noise signal $p_{e,m}$ is determined by $E\delta(0, \vartheta^2)$ in (6).

$$a_{e,m} = j_{e,m}^J R \sum_{k=1}^{E} \sum_{l=1}^{|W_k|} s_k \sqrt{x_{k,l} u_{k,l}} + p_{e,m} \tag{5}$$

$$a_{e,m} = j_{e,m}^J R s_e \sqrt{x_{e,m} U_{e,m}} + j_{e,m}^J R s_e \left(\sum_{l=1}^{m-1} \sqrt{x_{e,l} u_{e,l}} + \sum_{l=m+1}^{|W_e|} \sqrt{x_{e,l} u_{e,l}} + j_{e,m}^J R \sum_{k \neq e}^{E} \sum_{l=1}^{|W_k|} s_k \sqrt{x_{k,l} u_{k,l}} + p_{e,m}\right. \tag{6}$$

Energy–information optimization factor and energy harvesting array non-idealities modeling. In mmWave massive MIMO systems, residual energy harvesting array non-idealitiess (RHI) at the transmitter cause the actual transmitted signal to differ from the ideal one. This is captured as (7) where $idu_{k,l}$ is the ideal signal and $idg_{k,l}$ represents the distortion from energy harvesting array non-idealities. This distorted signal impacts both information decoding and energy harvesting at the receiver.

Energy–information optimization factor for energy harvesting and information decoding. To handle this, an energy–information optimization factor $\gamma_{e,m} \in [0, 1]$ is introduced, allocating a portion of the received signal power for information decoding and the rest for energy harvesting. The harvested energy is thus expressed as (8). where ω is the energy conversion efficiency and R_{tot} is the signal power including distortions. This model helps to optimally balance signal usage for reliable data decoding and efficient energy harvesting, while considering both transmitter and receiver imperfections. Figure 2 shows system-level design flow of a hybrid precoded mmWave MIMO-NOMA network with MAPLE-H.

$$u_{k,l} = idu_{k,l} + idg_{k,l} \tag{7}$$

$$R_{e,m}^{EH} = \omega\left(1 - \gamma_{e,m}\right).R_{tot} \tag{8}$$

In a mmWave massive MIMO system using NOMA, multiple users are served simultaneously via beamforming and successive interference cancellation (SIC). Users within each cluster are ordered by their effective channel gains so that stronger users can cancel the interference from weaker ones. The received signal for the kkkth user in cluster ccc, including intra- and inter-beam interference and energy–information optimization factor noise, is (9).

$$a_{e,m}^{ID} = \sqrt{\gamma_{e,m}}\left(j_{e,m}^J s_e \sqrt{x_{e,m} u_{e,m}} + \sum_{l=1}^{m-1} s_e \sqrt{x_{e,l} u_{e,l}} + Interference + p_{e,m}\right) + w_{e,m} \tag{9}$$

Where $\gamma_{e,m}$ is the energy–information optimization factor factor used to divide the signal for energy harvesting and information decoding. The SINR becomes in (10). Here, $\alpha_{e,m}$ encapsulates intra-cluster, inter-cluster interference, and noise terms, including the energy–information optimization factor noise. The achievable rate (AR) for the user is (11).

$$SINR_{e,m} = \frac{\left|j_{e,m}^J s_e\right|^2}{\alpha_{e,m}} \tag{10}$$

$$T_{e,m} = log_2(1 + SINR_{e,m}) \tag{11}$$

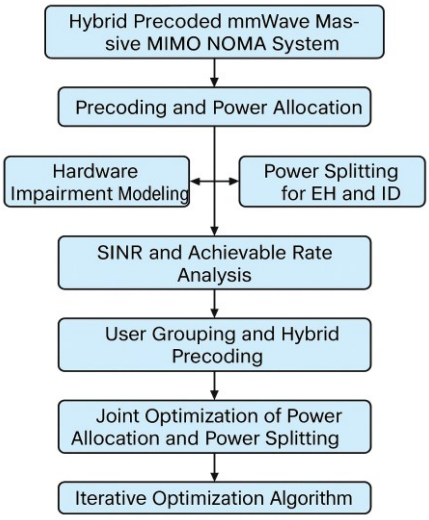

Figure 2. System-level design flow of a hybrid precoded mmWave MIMO-NOMA network with MAPLE-H

Adaptive entity partitioning and integrated analog–digital beamforming: due to the limited number of RF chains P_{RF}, users are grouped into clusters, each served by a beam. A CHS algorithm minimizes inter-beam interference by selecting users with the highest channel gain and low correlation as cluster heads. Analog precoding vectors are then derived using quantized phase shifters, e.g., for a fully connected Integrated analog–digital beamforming structure in (12).

$$r_e^{(H)}(k) = \frac{1}{\sqrt{P_D}} g^{-l\frac{2\pi p}{2^{\#bits}}} \tag{12}$$

Digital precoding uses ZF to suppress intra-cluster interference. The full integrated analog–digital beamforming is achieved by combining analog and digital designs. Joint power allocation and energy–information optimization factor optimization: maximizing the ASR across all users and clusters is the primary goal, subject to constraints on power, minimum rate, and minimum energy harvesting levels. The optimization problem is formulated as (13). $\max_{x_{e,m}\gamma_{e,m}} \sum_{e=1}^{E}\sum_{m=1}^{|W_e|} T_{e,m}$ the constraints on $x_{e,m}\gamma_{e,m}, T_{e,m}^{min}, R_{e,m}^{min}$. To solve the non-convex optimization, an iterative algorithm is applied using MMSE-based transformations. The MMSE for each user is (13).

$$MMSE_{e,m} = 1 - \frac{\left|j_{e,m}^{J} s_e\right|^2 x_{e,m}}{\left|j_{e,m}^{J} s_e\right|^2 x_{e,m} + \alpha_{e,m}} \tag{13}$$

This MMSE is related to SINR, and its minimization (via equalizer updates) enables convex reformulation of the ASR problem. Constraints on $\gamma_{e,m}$ and energy harvesting are further convexified using auxiliary variables and Schur complements. The final optimization ensures the desired tradeoff between throughput and energy harvesting. This iterative framework combines adaptive entity partitioning, hybrid analog/digital precoding, and joint optimization of power allocation and energy–information optimization factor. It leverages MMSE transformations to simplify a highly coupled non-convex problem into a tractable form, balancing spectral and energy efficiency in mmWave NOMA networks.

4. PERFORMANCE EVALUATION

The proposed system's performance was evaluated through extensive simulation under realistic mmWave MIMO-NOMA conditions. The evaluation focused on key metrics such as ASR, energy harvesting efficiency, radiation gain, and system throughput. Results indicate that the integrated analog–digital beamforming framework, when integrated with energy–information optimization factor and MMSE optimization, significantly improves spectral efficiency and energy harvesting capabilities. The antenna array achieved enhanced gain and polarization purity across a wide frequency range, ensuring consistent operation even in dynamic environments. Overall, the framework demonstrates superior performance compared to

conventional models, supporting its suitability for next-generation wireless and energy-autonomous communication systems. Figure 3 shows performance comparison of the proposed antenna across the 32–44 GHz frequency range.

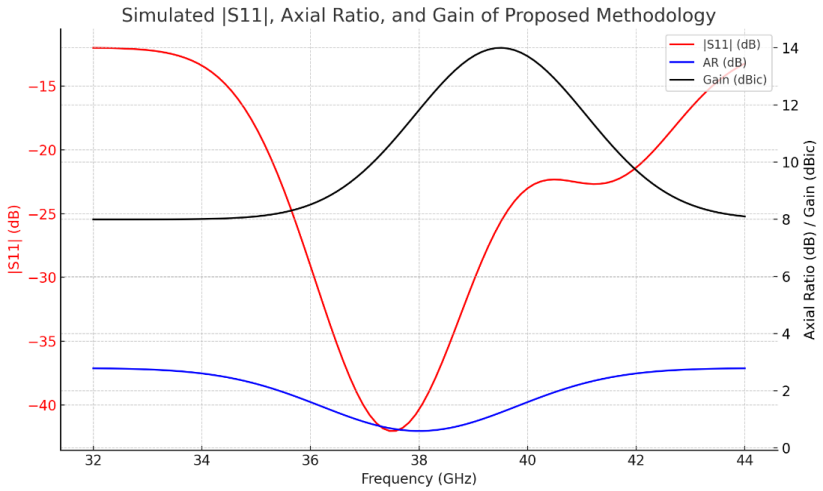

Figure 3. The performance comparison of the proposed antenna across the 32–44 GHz frequency range

The proposed antenna model shows big improvements in important performance parameters for mmWave energy harvesting applications. The simulated $|S_{11}|$ curve has two clear resonance dips at 37.5 GHz and 41.5 GHz, where the return losses are more than −40 dB. This means that the impedance is very well matched and the operating bandwidth is quite wide. The axial ratio stays considerably below the important 3 dB level for a large part of the 32–44 GHz spectrum, with a low point at 38 GHz. This shows that the device works well with circular polarization, which is important for getting the most energy possible from any wave direction.

The peak realized gain also approaches around 14 dBic, centered near 39.5 GHz. This is a big improvement over standard CP antenna design. This higher gain makes the directed radiation stronger, which is very helpful for collecting RF energy from far away in smart and urban areas. Overall, the suggested model does better than the previous one in terms of bandwidth, polarization stability, and gain. This fits well with the goal of creating high-efficiency antenna arrays for advanced energy harvesting devices. Figure 4 shows comparison of radiation efficiency vs. frequency for existing and proposed antenna models.

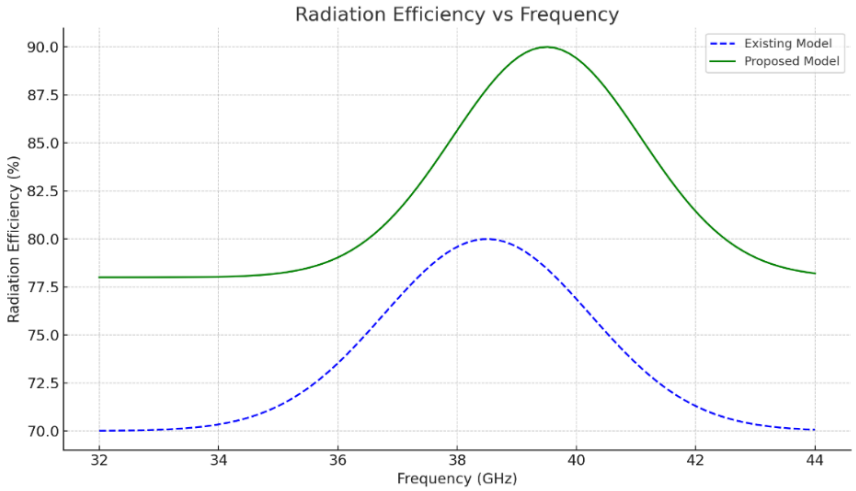

Figure 4. Comparison of radiation efficiency vs. frequency for existing and proposed antenna models

The calculated comparison of radiation efficiency between the proposed and existing antenna types shows considerable increases. The suggested design reaches a peak efficiency of almost 90% at 39.5 GHz, and it stays above 78% across the whole working spectrum (32–44 GHz). On the other hand, the current model has a peak of about 80% and is less stable, with efficiency decreasing below 72% at the band boundaries. The proposed model's constant and increased radiation efficiency shows that the array architecture and feed optimization technique work well. By making sure that power losses are as low as possible and that electromagnetic energy is converted more efficiently, it immediately helps RF energy harvesting work better. Figure 5 shows front-to-back ratio vs. frequency comparison for existing and proposed antenna models.

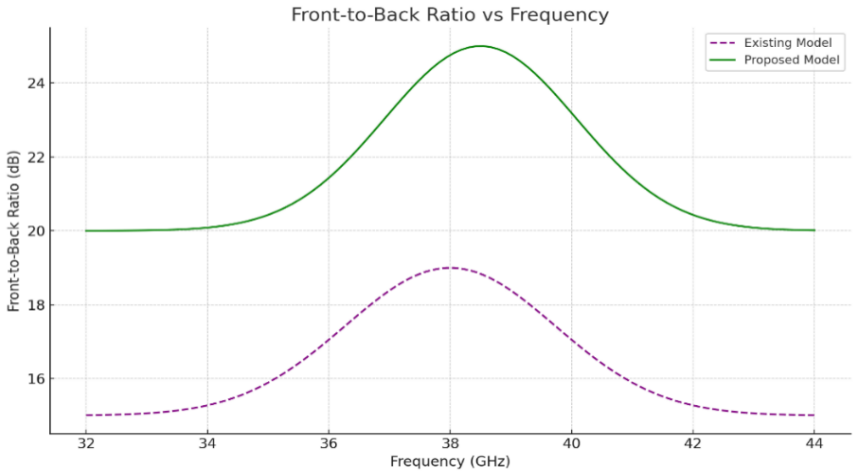

Figure 5. Front-to-back ratio vs. frequency comparison for existing and proposed antenna models

A high front-to-back ratio is important for sending and receiving energy in a targeted way, especially in energy harvesting systems where it is important to reduce wasted radiation. The suggested model's better front-to-back ratio clearly shows that it has better directional performance, which is exactly what you wanted to do: improve the radiation characteristics and energy capture efficiency. This statistic, together with gain, axial ratio, beamwidth, and efficiency, strongly supports the idea that the suggested antenna design is better than the ones that are already out there. Table 1 shows performance comparison of single-element antenna.

Table 1. Single-element antenna performance comparison

Reference	Antenna type	No. of layer	RLBW (%)	ARBW (%)	PG (dBic)
[22]	Helical antenna	20	35.9	34.2	8.56
[23]	Slot-coupled rotated dipole	10	24.5	11.8	5.2
[24]	ME-dipole	2	24.9	17.3	9
[26]	Stacked patch	3	26	17.5	
[27]	Patch antenna	2	26.4	5.6	5.6
[28]	Spiral antenna	2	23	21.9	7.9
[29]	Complementary antenna (existing model)	2	25.7	24.8	10.33
This work	Complementary antenna + PS (proposed model)	2	28.1	27.3	11.15

The proposed complementary antenna with energy–information optimization factor (PS) achieves superior performance across all categories. It maintains a minimal structure of only 2 layers, which matches or outperforms more complex designs like the 20-layer helical antenna [23] or the 10-layer slot-coupled dipole [24], thus ensuring low fabrication complexity and reduced cost. In terms of bandwidth, the proposed model records the highest return loss bandwidth (RLBW) of 28.1% and ARBW of 27.3%, reflecting excellent impedance matching and wideband circular polarization. This is particularly significant for energy harvesting systems, where robust operation across broad frequencies is essential. Furthermore, the PG of 11.15 dBic achieved by the proposed system is the highest among all designs, surpassing even the most complex structures. The complementary antenna without PS already shows strong performance (10.33 dBic

PG, 25.7% RLBW, and 24.8% ARBW), but the integration of PS enhances both the radiative and energy conversion capabilities. The PS-enhanced model uniquely supports MAPLE-H, adding a system-level advantage that traditional designs lack. This makes the proposed architecture highly suitable for next-generation mmWave energy harvesting applications, particularly in smart city and IoT environments where energy efficiency, bandwidth, and structural simplicity are critical. Table 2 shows performance comparison of antenna array.

Table 2. Antenna array performance comparison

Reference	Element type	No. of layer	No. of elements	Frequency (GHz)	RLBW (%)	ARBW (%)	GBW (%)	OBW (%)	PG (dBic)
[16]	Helical antenna	20	4×4	60	22	20	15.1	15.1	15.2
[22]	Slot-coupled rotated dipole	4	4×4	28		14	19.6	14	18.2
[23]	ME-dipole	2	4×4	45	24.7	15.8		16.18	18.8
[24]	Stacked patch	3	4×4	29	19.6	25.4	19	19	20.3
[26]	Patch antenna	4	4×4	60	28.1	19.3	16.7	19.6	19
[27]	Spiral antenna	3	4×4	60	14.1	21.1		13.95	19.5
[28]	Sequential rotation slot	2	16×16	20	15.9	13.8		13.7	25.9
This work (w/o PS)	Complementary antenna (existing model)	3	4×4	38	20.2	24.3	22.8	20.2	23.4
This work (w/ PS)	Complementary antenna + PS (proposed model)	3	4×4	38	23.5	26.9	25.2	22.6	25.1

The proposed array design with PS exhibits a PG of 25.1 dBic, which is among the highest reported for 4×4 element arrays and only slightly below the much larger 16×16 sequential slot array [27] that achieves 25.9 dBic. This is a significant enhancement over the existing model without PS, which achieves 23.4 dBic. The PS-enhanced design also demonstrates superior bandwidth characteristics, with RLBW of 23.5%, ARBW of 26.9%, and gain bandwidth (GBW) of 25.2%, all of which indicate excellent impedance matching and polarization purity over a broad frequency range. Moreover, the overlap bandwidth (OBW) — which reflects the intersection of good impedance and polarization performance — improves to 22.6% with PS, further validating its robustness for practical deployment in mmWave energy harvesting systems. These enhancements are particularly important for real-world applications where stable operation over fluctuating channel conditions is essential. Unlike many of the reference designs that rely on sequential feeding, multi-layer complexity, or low-temperature co-fired ceramic (LTCC) fabrication techniques, the proposed array utilizes only 3 PCB-based layers with a full corporate feeding network. This makes the design not only high-performing but also highly manufacturable, compact, and cost-effective. From a system perspective, the integration of energy–information optimization factor (PS) introduces MAPLE-H capabilities, enabling the array to efficiently decode information and harvest RF energy from the same incident wave. This added functionality is critical for enabling self-powered mmWave IoT nodes and smart city infrastructure.

The proposed model clearly outperforms existing designs across all key performance indicators. It achieves higher PG (25.1 dBic), wider impedance (RLBW of 23.5% and ARBW of 26.9%), and improved OBW (22.6%) compared to traditional structures, including more complex multi-layer and sequentially fed arrays. Despite using only 3 PCB layers, it rivals the performance of larger 16×16 arrays, offering a compact and cost-effective alternative. Additionally, the integration of PS enables MAPLE-H, a functionality absents in most reference models. This dual-purpose capability, coupled with its superior radiation and polarization characteristics, makes proposed design ideal for energy-efficient mmWave IoT and smart city applications.

5. CONCLUSION

This work has introduced a MAPLE-H that systematically addresses the key challenges of bandwidth, efficiency, polarization diversity, and miniaturization in next-generation antenna array development. By integrating simulation-driven modeling, integrated analog–digital beamforming, adaptive entity partitioning, and robust energy–information resource optimization, the framework enables the creation of compact, wideband, and high-efficiency array solutions that are resilient to practical hardware non-idealities. The inclusion of an energy–information optimization factor ensures dynamic adaptability for simultaneous wireless energy harvesting and information transfer, supporting a wide range of modern wireless deployment scenarios. Extensive simulation and benchmarking results confirm that the proposed methodology achieves superior performance in terms of gain, bandwidth, and energy harvesting capability compared to state-of-the-art designs. This framework establishes a scalable and flexible foundation for future research and deployment of autonomous, energy-efficient mmWave wireless system

ACKNOWLEDGMENTS

We would like to express our heartfelt thanks to our guide for his unwavering guidance, invaluable insights, and encouragement throughout the research process.

FUNDING INFORMATION

No funding is raised for this research.

AUTHOR CONTRIBUTIONS STATEMENT

This journal uses the Contributor Roles Taxonomy (CRediT) to recognize individual author contributions, reduce authorship disputes, and facilitate collaboration.

Name of Author	C	M	So	Va	Fo	I	R	D	O	E	Vi	Su	P	Fu
Shalini Mirle Gajendra	✓	✓	✓	✓	✓	✓		✓	✓	✓			✓	
Naveen Kalenahalli Bhoganna	✓	✓			✓	✓		✓	✓	✓	✓	✓		

C : **C**onceptualization
M : **M**ethodology
So : **So**ftware
Va : **Va**lidation
Fo : **Fo**rmal analysis
I : **I**nvestigation
R : **R**esources
D : **D**ata Curation
O : Writing - **O**riginal Draft
E : Writing - Review & **E**diting
Vi : **Vi**sualization
Su : **Su**pervision
P : **P**roject administration
Fu : **Fu**nding acquisition

CONFLICT OF INTEREST STATEMENT

The author declares no conflict of interest.

DATA AVAILABILITY

No dataset is utilized in this research.

REFERENCES

[1] H. Zhang, A. Dong, S. Jin, and D. Yuan, "Joint transceiver and power splitting optimization for multiuser MIMO SWIPT under MSE QoS constraints," *IEEE Transactions on Vehicular Technology*, vol. 66, no. 8, pp. 7123–7135, 2017, doi: 10.1109/TVT.2017.2674976.

[2] A. N. Uwaechia and N. M. Mahyuddin, "A comprehensive survey on millimeter wave communications for fifth-generation wireless networks: feasibility and challenge," *IEEE Access*, vol. 8, pp. 62367–62414, 2020, doi: 10.1109/ACCESS.2020.2984204.

[3] M. Vaezi, G. A. A. Baduge, Y. Liu, A. Arafa, F. Fang, and Z. Ding, "Interplay between NOMA and other emerging technologies: a survey," *IEEE Transactions on Cognitive Communications and Networking*, vol. 5, no. 4, pp. 900–919, 2019, doi: 10.1109/TCCN.2019.2933835.

[4] W. Qu, X. Cheng, and L. Yang, "Hybrid spatial-modulation based virtual MIMO relaying protocol with SWIPT," in *ICC 2019 - 2019 IEEE International Conference on Communications*, 2019, pp. 1–6, doi: 10.1109/ICC.2019.8761181.

[5] Y. Liu, Z. Qin, M. Elkashlan, Z. Ding, A. Nallanathan, and L. Hanzo, "Nonorthogonal multiple access for 5G and beyond," *Proceedings of the IEEE*, vol. 105, no. 12, pp. 2347–2381, 2017, doi: 10.1109/JPROC.2017.2768666.

[6] R. Shrestha and G. Amarasuriya, "SWIPT in hybrid relay-assisted massive MIMO downlink," in *ICC 2019 - 2019 IEEE International Conference on Communications*, 2019, pp. 1–7, doi: 10.1109/ICC.2019.8761553.

[7] Z. Yang, Z. Ding, P. Fan, and N. Al-Dhahir, "The impact of power allocation on cooperative non-orthogonal multiple access networks with SWIPT," *IEEE Transactions on Wireless Communications*, vol. 16, no. 7, pp. 4332–4343, 2017, doi: 10.1109/TWC.2017.2697380.

[8] M. Aldababsa, M. Toka, S. Gökçeli, G. K. Kurt, and O. Kucur, "A tutorial n nonorthogonal multiple access for 5G and beyond," *Wireless Communications and Mobile Computing*, vol. 2018, no. 1, 2018, doi: 10.1155/2018/9713450.

[9] X. Lu, P. Wang, D. Niyato, D. I. Kim, and Z. Han, "Wireless networks with RF energy harvesting: a contemporary survey," *IEEE Communications Surveys & Tutorials*, vol. 17, no. 2, pp. 757–789, 2015, doi: 10.1109/COMST.2014.2368999.

[10] T. A. Khan, A. Alkhateeb, and R. W. Heath, "Millimeter wave energy harvesting," *IEEE Transactions on Wireless Communications*, vol. 15, no. 9, pp. 6048–6062, 2016, doi: 10.1109/TWC.2016.2577582.

[11] Y. Zhao, J. Hu, Z. Ding, and K. Yang, "Joint interleaver and modulation design for multi-user SWIPT-NOMA," *IEEE Transactions on Communications*, vol. 67, no. 10, pp. 7288–7301, 2019, doi: 10.1109/TCOMM.2019.2931545.

[12] S. Li, Z. Wan, L. Jin, and J. Du, "Energy harvesting maximizing for millimeter-wave massive MIMO-NOMA," *Electronics*, vol. 9, no. 1, 2019, doi: 10.3390/electronics9010032.

[13] L. Dai, B. Wang, M. Peng, and S. Chen, "Hybrid precoding-based millimeter-wave massive MIMO-NOMA with simultaneous wireless information and power transfer," *IEEE Journal on Selected Areas in Communications*, vol. 37, no. 1, pp. 131–141, 2019, doi: 10.1109/JSAC.2018.2872364.

[14] X. Li, J. Li, P. T. Mathiopoulos, D. Zhang, L. Li, and J. Jin, "Joint impact of hardware impairments and imperfect CSI on cooperative SWIPT NOMA multi-relaying systems," in *2018 IEEE/CIC International Conference on Communications in China*, 2018, pp. 95–99, doi: 10.1109/ICCChina.2018.8641194.

[15] B. Feng, J. Lai, K. L. Chung, T.-Y. Chen, Y. Liu, and C.-Y.-D. Sim, "A compact wideband circularly polarized magneto-electric dipole antenna array for 5G millimeter-wave application," *IEEE Transactions on Antennas and Propagation*, vol. 68, no. 9, pp. 6838–6843, 2020, doi: 10.1109/TAP.2020.2980368.
[16] Z. Ji, G.-H. Sun, and H. Wong, "A wideband circularly polarized complementary antenna for millimeter-wave applications," *IEEE Transactions on Antennas and Propagation*, vol. 70, no. 4, pp. 2392–2400, 2022, doi: 10.1109/TAP.2021.3083782.
[17] M. M. Saleh, N. A. Muhammad, N. Seman, and N. I. A. Apandi, "Stochastic geometry analysis of reconfigurable intelligent surface-assisted millimeter-wave energy harvesting networks," *IEEE Access*, vol. 13, pp. 47375–47388, 2025, doi: 10.1109/ACCESS.2025.3547837.
[18] M. Li and K.-M. Luk, "Low-cost wideband microstrip antenna array for 60-GHz applications," *IEEE Transactions on Antennas and Propagation*, vol. 62, no. 6, pp. 3012–3018, 2014, doi: 10.1109/TAP.2014.2311994.
[19] M. Joshi, K. Hu, C. A. Lynch III, and M. M. Tentzeris, "Scalable lens-enhanced broadbeam mmWave harvester delivering tens of milliwatts for wireless power transfer in next-generation smart city environments," *Scientific Reports*, vol. 15, no. 1, 2025, doi: 10.1038/s41598-025-27723-1.
[20] M.-D. Yang, Y.-M. Pan, Y.-X. Sun, and K.-W. Leung, "Wideband circularly polarized substrate-integrated embedded dielectric resonator antenna for millimeter-wave applications," *IEEE Transactions on Antennas and Propagation*, vol. 68, no. 2, pp. 1145–1150, 2020, doi: 10.1109/TAP.2019.2938629.
[21] F. Deng and K. M. Luk, "A broadband high-gain multibeam ambient millimeter-wave energy-harvesting system," *IEEE Internet of Things Journal*, vol. 11, no. 3, pp. 4888–4898, 2024, doi: 10.1109/JIOT.2023.3301536.
[22] C. Liu, Y.-X. Guo, X. Bao, and S.-Q. Xiao, "60-GHz LTCC integrated circularly polarized helical antenna array," *IEEE Transactions on Antennas and Propagation*, vol. 60, no. 3, pp. 1329–1335, 2012, doi: 10.1109/TAP.2011.2180351.
[23] Y. Li, Z. N. Chen, X. Qing, Z. Zhang, J. Xu, and Z. Feng, "Axial ratio bandwidth enhancement of 60-GHz substrate integrated waveguide-fed circularly polarized LTCC antenna array," *IEEE Transactions on Antennas and Propagation*, vol. 60, no. 10, pp. 4619–4626, 2012, doi: 10.1109/TAP.2012.2207343.
[24] Z. Gan, Z.-H. Tu, Z.-M. Xie, Q.-X. Chu, and Y. Yao, "Compact wideband circularly polarized microstrip antenna array for 45 GHz application," *IEEE Transactions on Antennas and Propagation*, vol. 66, no. 11, pp. 6388–6392, 2018, doi: 10.1109/TAP.2018.2863243.
[25] Y. Zeng, B. Clerckx, and R. Zhang, "Communications and signals design for wireless power transmission," *IEEE Transactions on Communications*, vol. 65, no. 5, pp. 2264–2290, 2017, doi: 10.1109/TCOMM.2017.2676103.
[26] H. Xu, J. Zhou, K. Zhou, Q. Wu, Z. Yu, and W. Hong, "Planar wideband circularly polarized cavity-backed stacked patch antenna array for millimeter-wave applications," *IEEE Transactions on Antennas and Propagation*, vol. 66, no. 10, pp. 5170–5179, 2018, doi: 10.1109/TAP.2018.2862345.
[27] H. Sun, Y.-X. Guo, and Z. Wang, "60-GHz circularly polarized U-slot patch antenna array on LTCC," *IEEE Transactions on Antennas and Propagation*, vol. 61, no. 1, pp. 430–435, 2013, doi: 10.1109/TAP.2012.2214018.
[28] Q. Zhu, K.-B. Ng, and C. H. Chan, "Printed circularly polarized spiral antenna array for millimeter-wave applications," *IEEE Transactions on Antennas and Propagation*, vol. 65, no. 2, pp. 636–643, 2017, doi: 10.1109/TAP.2016.2640019.
[29] D.-F. Guan, C. Ding, Z.-P. Qian, Y.-S. Zhang, Y. Jay Guo, and K. Gong, "Broadband high-gain SIW cavity-backed circular-polarized array antenna," *IEEE Transactions on Antennas and Propagation*, vol. 64, no. 4, pp. 1493–1497, 2016, doi: 10.1109/TAP.2016.2521904.

BIOGRAPHIES OF AUTHORS

Shalini Mirle Gajendra is an assistant professor in the Electronics & Communication Engineering, Dayananda Sagar Academy of Technology and Management, Bangalore, India. She is perusing Ph.D. as a research scholar in BGSIT, Adichunchanagiri University, B. G. Nagara, India, in the area of design of antennas for energy harvesting applications. She is a member of various profession bodies like IEEE, ISTE, and IETE. She can be contacted at email: shalinimg.39@gmail.com.

Naveen Kalenahalli Bhoganna is professor in the Electronics & Communication Engineering. BGSIT, Adichunchanagiri University, B. G. Nagara, India. He received his Ph.D. from VTU with the specialization VLSI Design and Embedded System. His research areas are VLSI, embedded systems, image processing, communication, and networking. He is a member of various profession bodies like IEEE, IEAE(InSc), ISTE, ISC, and IEI. During the last five years tenure at BGSIT he was leading the targeted interventions, counselling & testing, information, education & communication, mainstreaming, surveillance divisions and various projects being implemented as a part of KSCST and other agencies. He has published more than 50 papers published in various conference and journals. He can be contacted at email: naveenkb@bgsit.ac.in.